

On the dynamics of edge-core coupling

T. S. Hahm^{a)}

Princeton Plasma Physics Laboratory, Princeton University, Princeton, New Jersey 08543

P. H. Diamond

University of California San Diego, La Jolla, California 92093 and Research Institute for Applied Mechanics, Kyushu University, Kasuga 816, Japan

Z. Lin

University of California Irvine, Irvine, California 92697

G. Rewoldt

Princeton Plasma Physics Laboratory, Princeton University, Princeton, New Jersey 08543

O. Gurcan

University of California San Diego, La Jolla, California 92093

S. Ethier

Princeton Plasma Physics Laboratory, Princeton University, Princeton, New Jersey 08543

(Received 18 March 2005; accepted 16 May 2005; published online 21 September 2005)

One of the nagging, unresolved questions in fusion theory is concerned with the extent of the edge. Gyrokinetic particle simulations of toroidal ion temperature gradient turbulence spreading using the gyrokinetic toroidal code [Z. Lin, T. S. Hahm, W. W. Lee, W. M. Tang, and R. B. White, *Science* **281**, 1835 (1998)] and its related dynamical model have been extended to a system with radially varying ion temperature gradient, in order to study the inward spreading of edge turbulence toward the core plasma. Due to such spreading, the turbulence intensity in the core region is significantly enhanced over the value obtained from the simulations of the core region only, and the precise boundary of the edge region is blurred. Even when the core gradient is within the Dimits shift regime (i.e., dominated by self-generated zonal flows which reduce the transport to a negligible value), a significant level of turbulence can penetrate to the core due to spreading from the edge. The scaling of the turbulent front propagation speed is closer to the prediction from a nonlinear diffusion model than from the one based on linear toroidal coupling. © 2005 American Institute of Physics. [DOI: 10.1063/1.2034307]

I. INTRODUCTION

Despite significant progress in experiment, theory, and computation in recent years, the predictive capability of turbulence and transport modeling for magnetically confined plasmas is generally limited to case-by-case direct numerical simulations. One of the biggest obstacles to achieving a predictive capability is understanding edge turbulence and, specifically, the dynamics of edge-core interaction and coupling. This issue is especially crucial to understanding the formation and extent of the H -mode pedestal. In particular, the location of the edge-core boundary is both uncertain and dynamic (and usually posited in an *ad hoc* manner in transport codes), so that turbulence spreading surely plays a role in defining its location. Thus, serious challenges remain due to the fact that virtually all models of fluctuation levels and turbulent transport are built on an assumption of *local balance* of linear growth with linear damping and nonlinear coupling to dissipation, i.e., the traditional “local balance” paradigm of Kadomtsev.¹ Such models thus necessarily exclude mesoscale dynamics, which refers to dynamics on scales larger than a mode or integral scale eddy size, but smaller than the system. In particular, zonal flows, transport

barriers, avalanches, heat, and particle pulses are all mesoscale phenomena.^{2–7} Similarly, the dynamic or fluid nature of the edge-core boundary interface is intrinsically a mesoscale phenomenon. Such mesoscale phenomenon necessarily introduces an element of nonlocal interaction, which is also strongly suggested by several experiments, but conspicuously absent from the so-called predictive models.

In our previous studies,^{8,9} we have identified and studied in depth the simplest nontrivial problem of turbulence spreading, which corresponds to the spatiotemporal propagation of a patch of turbulence from a region where it is locally excited to a region of weaker excitation, or even one with local damping. Our published results focusing on the importance of growth and damping rate profiles in the spatiotemporal evolution of turbulence are in a broad, semiquantitative agreement with the global gyrokinetic simulations of (core) ion temperature gradient (ITG) turbulence.^{9,10} In particular, it has been demonstrated that turbulence spreading into the linearly stable zone can cause deviation of the transport scaling from the gyro-Bohm scaling naively expected from the local characteristics of turbulence. From these observations, it seems likely that turbulence spreading plays a crucial role in determining turbulence and transport profiles in the core-edge connection region where the gradient increases rapidly

^{a)}Electronic mail: tshahm@pppl.gov

as a function of radius. Alternatively put, since an L -mode edge is very strongly turbulent, and since spatiotemporal spreading and propagation of turbulence are natural aspects of the dynamics, it is logical to consider the possibility of backwash or spillover from the edge into the core.

Turbulence propagation and overshoot vitiate the naive picture of turbulent transport based upon local balance, which is assumed in virtually all modeling codes. Moreover, energy propagation from the strongly turbulent edge into the core can effectively renormalize the edge “boundary condition” used in the modeling calculation. This ultimately feeds into the predictions of pedestal extent and into the so-called “edge boundary conditions” used in modeling codes.

II. GYROKINETIC SIMULATION OF TURBULENCE SPREADING FROM EDGE

In this paper, a program of numerical experiments is discussed. This aims to elucidate and study the inward propagation of turbulence from the L -mode edge into the core. This propagation generates a connection zone between the edge and core, which may be construed as a symptom of the oft referred to but ill-defined “nonlocality phenomena.” We focus our studies on the simple case with an ion temperature gradient which increases rapidly with increasing r , so as to study the inward spreading of edge turbulence toward the core. We note that the possibility of edge turbulence influencing core turbulence has been discussed before.^{11,12} Our main computational tool is a well-benchmarked, massively parallel, full torus gyrokinetic toroidal code (GTC).¹³ Toroidal geometry is treated rigorously, e.g., the radial variations of safety factor q , magnetic shear \hat{s} , and trapped particle fraction are retained in global simulations. Both linear and nonlinear wave-particle resonances and finite Larmor radius effects are included in gyrokinetic particle simulations. GTC employs magnetic coordinates which provide the most general coordinate system for any magnetic configuration possessing nested surfaces. The global field-aligned mesh provides a high computational efficiency without any simplification in terms of physics models or simulation geometry. Unlike quasiloc codes in flux-tube geometry which remove important radial variations of key equilibrium quantities, such as safety factor, magnetic shear, and temperature gradient, and use periodic boundary conditions in the radial direction, GTC does not rely on the ballooning mode formalism which becomes dubious in describing mesoscale phenomena including turbulence spreading.

All simulations reported in this paper use representative parameters of tokamak plasmas¹⁴ with the following local parameters at $r/a=0.5$: $R_0/L_n=2.2$, $q=1.4$, and $\hat{s}\equiv(r/q)\times(dq/dr)=0.78$, with $T_e/T_i=1$ and $a/R_0=0.36$. Here R_0 is the major radius, a is the minor radius, L_{Ti} and L_n are the ion temperature and density gradient scale lengths, respectively, T_i and T_e are the ion and electron temperatures, and q is the safety factor. Our global simulations use fixed boundary conditions with electrostatic potential $\delta\phi=0$ enforced at $r<0.1a$ and $r>0.9a$. Simplified physics models include a parabolic profile of $q=0.854+2.184(r/a)^2$. The temperature gradient profile mainly consists of two regions, a “core re-

gion” from $r/a=0.2$ to 0.5 , and an “edge region” from $r/a=0.5$ to 0.8 and a gradual decrease to much smaller values toward $r/a=0.1$ and $r/a=0.9$. A circular cross section and electrostatic fluctuations with adiabatic electron response are used in the simulations discussed in this paper. While this simple ITG turbulence does not apply directly as an edge turbulence model, it can elucidate dynamics of turbulence spreading.

The ion temperature gradient value in the core is based on our previous studies. In the first case summarized in Fig. 1, $R/L_{Ti}=6.9$ in the core, which is above the effective critical gradient in the presence of zonal flows $R/L_{crit}=6.0$, while in the second case summarized in Fig. 2, $R/L_{Ti}=5.3$ is within the Dimits shift regime.¹⁴ We double the value of the ion temperature gradient at the edge to model the stronger gradient at the tokamak edge. We have adopted this two-step feature for the ion temperature gradient to make comparisons with our previous core simulations^{9,15} and with an analytic model¹⁶ readily feasible.

Figure 1 shows the spatiotemporal evolution of the ITG turbulence envelope for the first case with $R/L_{Ti}=6.9$ in the core. The simulation ran until $t=300L_{Ti}/c_s$ when the turbulence apparently ceases to spread further. The initial growth in the edge region with $R/L_{Ti}=13.8$ and a higher linear growth rate is apparent from Figs. 1(a) and 1(b). By the time the edge turbulence saturates at $t\sim 200L_{Ti}/c_s$, turbulence spreading toward the core is already well in progress. The turbulence spreading can be characterized by nearly ballistic ($\sim t$) propagation of the front with a velocity $U_x\approx 2.6(\rho_i/R)c_s$. The time-average value of fluctuation intensity during the last 1/3 of the simulation duration at $r=0.4a$ (core) is $I\sim 36.5(\rho_i/a)^2$, which is about 60% above the value $I\sim 22.0(\rho_i/a)^2$ given by the core-only simulation with a maximum gradient $R/L_{Ti}=6.9$.⁹ In this case, the influx of edge turbulence energy from the edge into the core is comparable to the local growth of core turbulence.

Figure 2 shows the spatiotemporal evolution of the ITG turbulence envelope for the second case with $R/L_{Ti}=5.3$ in the core. The simulation ran until $t=500L_{Ti}/c_s$ when the turbulence apparently ceased to spread further. The initial growth in the edge region with $R/L_{Ti}=10.6$ and a higher linear growth rate is apparent from Figs. 2(a) and 2(b). By the time the edge turbulence saturates at $t\sim 300L_{Ti}/c_s$, turbulence spreading toward the core is already well under way, though the core region is effectively stable (i.e., within the Dimits shift regime) due to self-generated zonal flows. Note that at least in this case, the relaxation process which drives turbulence spreading is strong enough to overcome the stabilizing effects of the zonal flow shear. The evolving turbulence profile is better characterized by an exponential decay in space (with a characteristic “skin depth” $\sim 25\rho_i$ as we reported before in the context of core simulations^{8,9}) rather than by the shape of a propagating front. The time-average value of the fluctuation intensity during the last 1/3 of the simulation duration at $r=0.4a$ (core) is $I\sim 12.7(\rho_i/a)^2$, which translates to an experimentally relevant value of $\delta n/n_0\sim 3.6\rho_i/a$. We emphasize that the observed quasistationary fluctuation level in this region is driven primarily by the inward propagation of fluctuation energy from the

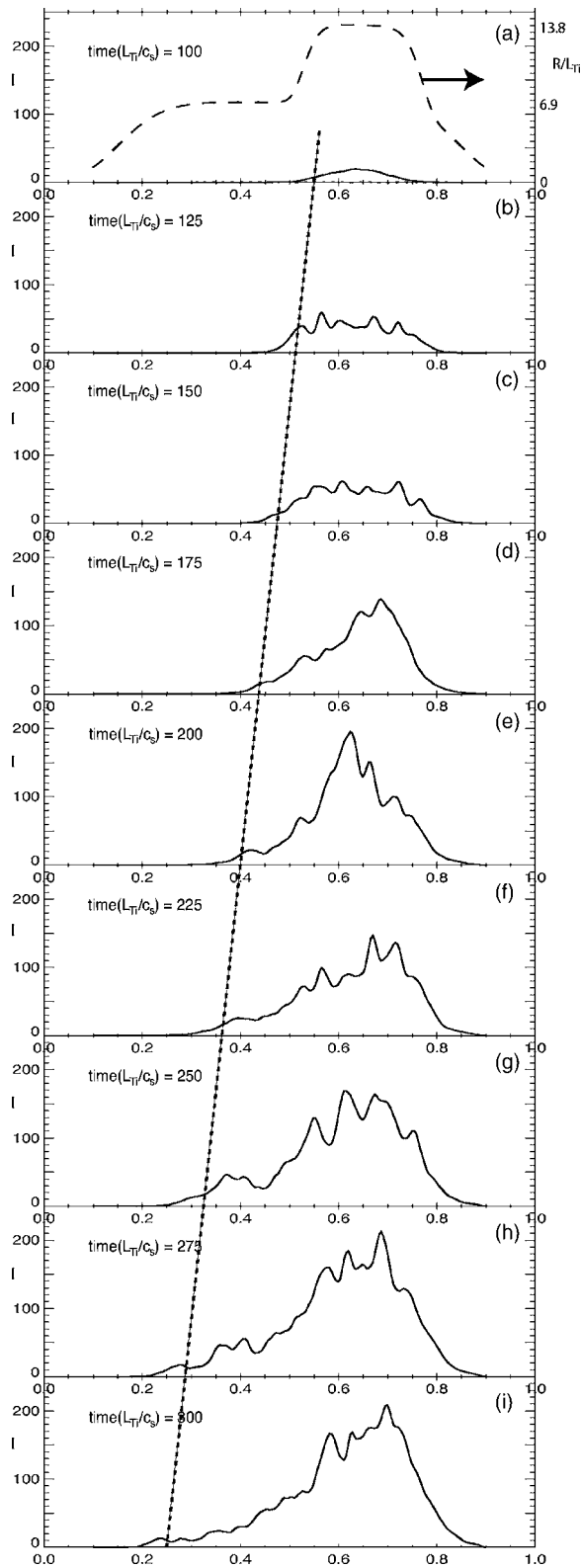


FIG. 1. Spatiotemporal evolution of the turbulence intensity from GTC simulation for $R/L_{Ti}=6.9$ in the core and 13.8 in the edge.

strongly turbulent edge, since the core simulation with a maximum gradient $R/L_T=5.3$ would have yielded a fluctuation level near zero, in the absence of collisional damping of the zonal flows.¹⁵ We have also performed a GTC nonlinear simulation for $R/L_{Ti}=9.0$ in the core and $R/L_{Ti}=18.0$ in the

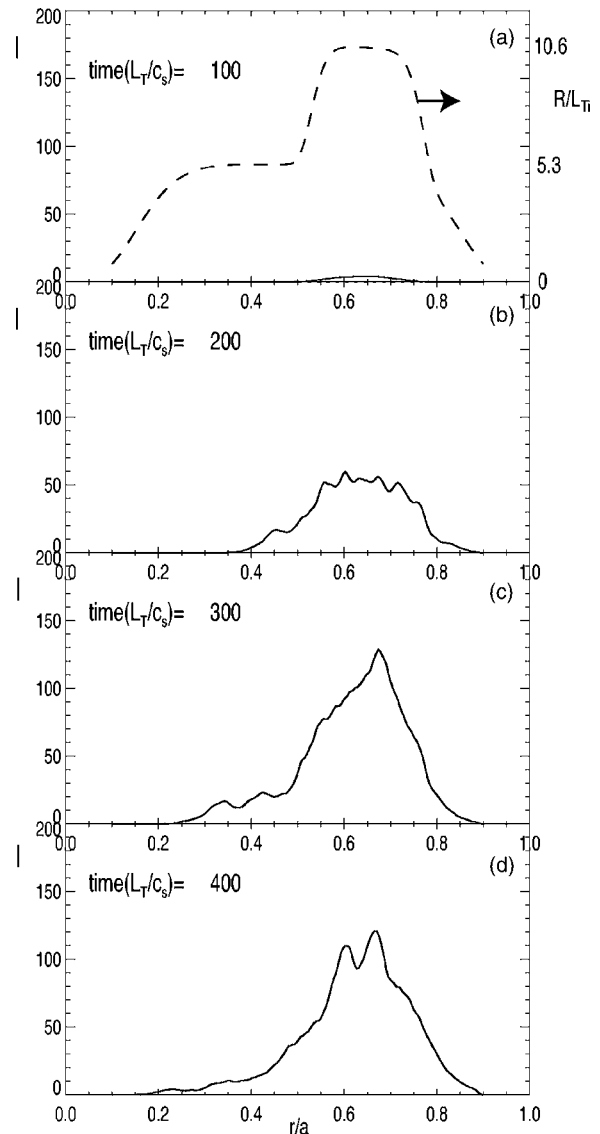


FIG. 2. Spatiotemporal evolution of the turbulence intensity from GTC simulation for $R/L_{Ti}=5.3$ in the core and 10.6 in the edge.

edge, and for $R/L_{Ti}=6.1$ in the core and $R/L_{Ti}=12.2$ in the edge. As shown in Figs. 3 and 4, the results are qualitatively similar to the case in Fig. 1 with $R/L_{Ti}=6.9$ in the core. The front propagation velocity was $U_x \approx 4.2(\rho_i/R)c_s$ and $U_x \approx 2.1(\rho_i/R)c_s$ for $R/L_{Ti}=9.0$ and $R/L_{Ti}=6.1$ in the core, respectively. The time-average value of the fluctuation intensity during the last 1/3 of the simulation duration at $r=0.4a$ (core) was $I \sim 65.1(\rho_i/a)^2$ and $I \sim 22.9(\rho_i/a)^2$, for $R/L_{Ti}=9.0$ and $R/L_{Ti}=6.1$ in the core, respectively. Since the spatiotemporal evolution of the fluctuation profiles are accompanied by relatively small-scale corrugations, we have estimated the “front propagation velocity” by displaying the snapshots, separated by equal time steps, and by drawing a straight line, by eye, through the “knees” which are apparent symptomatics of the propagating front.

In particular, previous related work has demonstrated that the intensity evolution equation is a modified Fischer-type reaction diffusion equation. Fischer equations are known to support front solutions, in which a “leading edge”

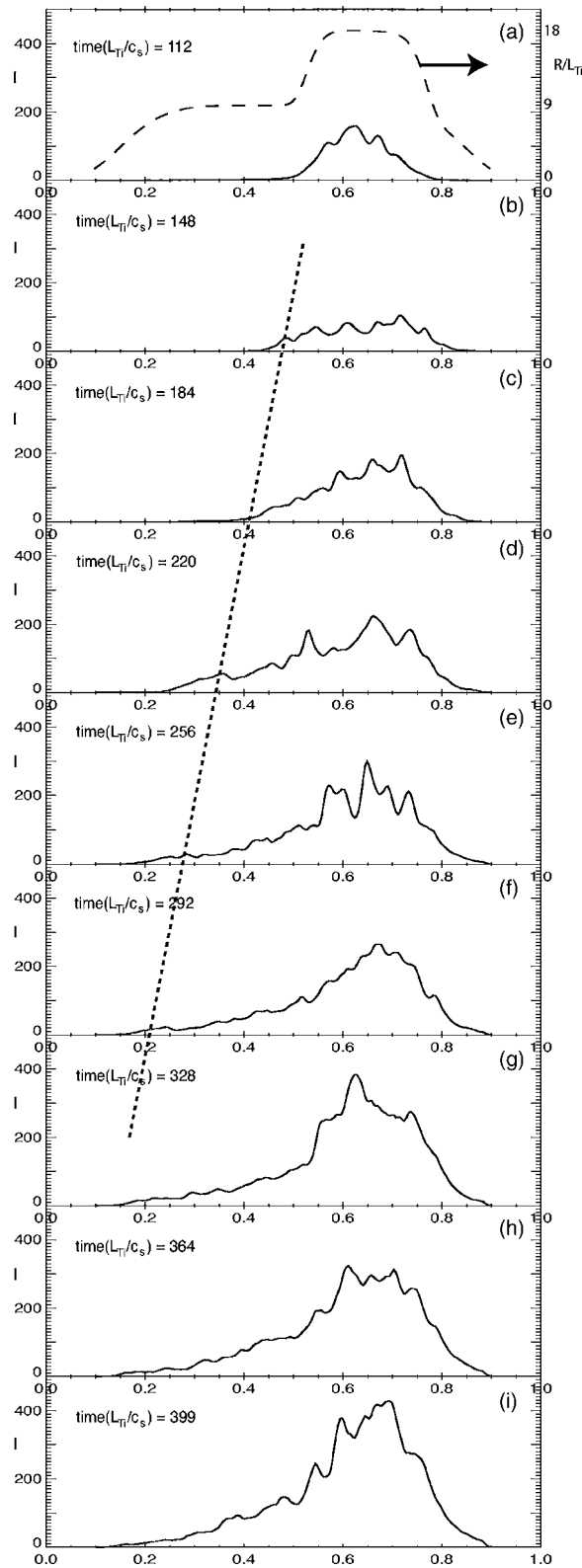


FIG. 3. Spatiotemporal evolution of the turbulence intensity from GTC simulation for $R/L_{Ti}=9.0$ in the core and 18.0 in the edge.

of one phase advances into the other. The leading edge is a region of decaying exponential, which ultimately joins to a region of constant order parameter. This connection necessitates the existence of an *inflection point* in the solution. The inflection point, in turn, sits at the *knee* of the profile. Thus,

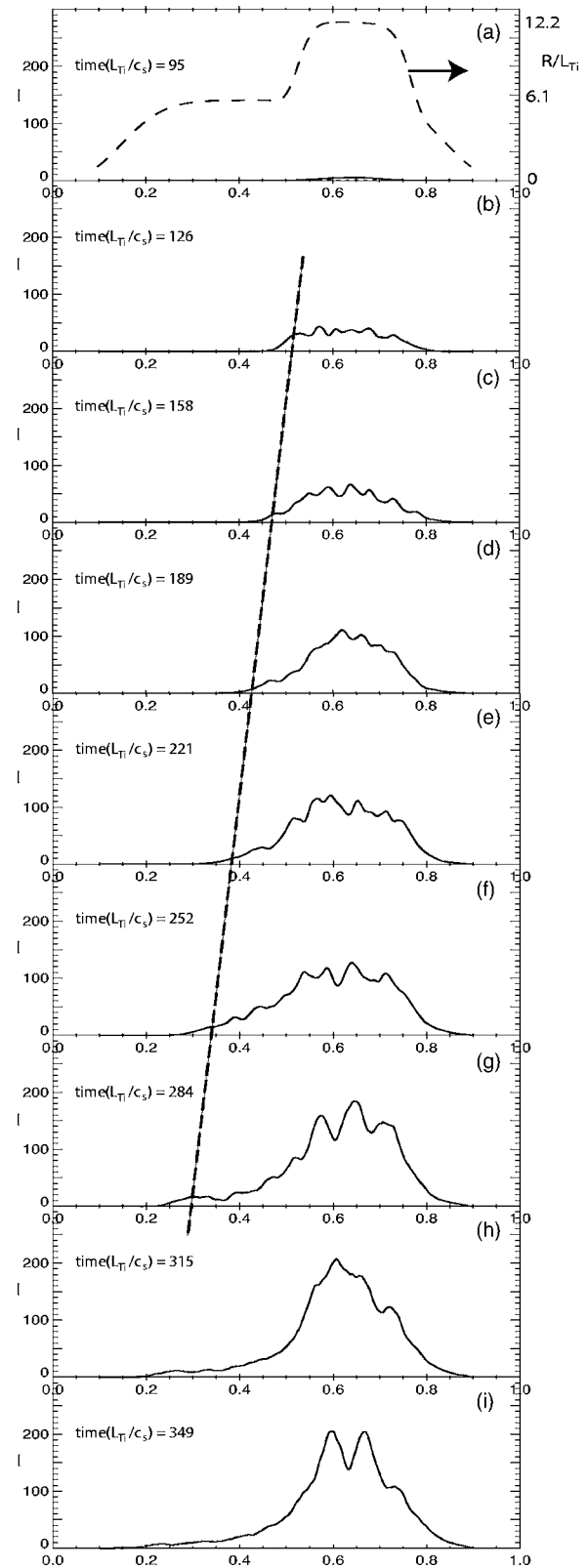


FIG. 4. Spatiotemporal evolution of the turbulence intensity from GTC simulation for $R/L_{Ti}=6.1$ in the core and 12.2 in the edge.

in order to relate simulation results to the theoretical models discussed here and in previous papers, it is natural and logical to track the location of the fluctuation intensity front by tracking the position of the knee in the intensity profile. Of

course, this is the crudest possible procedure, and a detailed quantitative fit to the simulation data is necessary for a more accurate comparison of theory and simulation.

III. ANALYTIC THEORY OF TURBULENCE SPREADING FROM THE EDGE

Our analytic study of turbulence spreading is based on a model equation for the local turbulence intensity $I(x, t)$, which includes the effects of local linear growth and damping, spatially local nonlinear coupling to dissipation, and spatial scattering of turbulence energy induced by nonlinear coupling:^{8,16,17}

$$\frac{\partial I}{\partial t} = \frac{\partial}{\partial x} \chi(I) \frac{\partial I}{\partial x} + \gamma(x) I - \alpha I^{1+\beta}. \quad (1)$$

The terms on the right-hand side correspond to nonlinear spatial scattering [i.e., typically $\chi(I) \sim \chi_0 I^\beta$ where $\beta=1$ for weak turbulence, and $\beta=1/2$ for strong turbulence], linear growth and damping, and local nonlinear decay, respectively. Here α is a nonlinear coupling coefficient. Note that α and χ_0 could be functions of radius. This equation is the irreducible minimum of the model. This equation has been derived from a Fokker–Planck-type analysis of the evolution of the turbulence intensity field in space (i.e., assuming a random walk of intensity with a step size equal to the integral scale and a time step equal to the correlation time).¹⁶ The walk yields the nonlinear diffusion term, while local evolution is described by the growth and nonlinear decay terms. In this respect, the model equation is similar to a type of K - ϵ model^{18,19} (or, more accurately, a K model) for the turbulence intensity field used in subgrid-scale modeling. Possible extensions of our model include the additional equations for other fields,²⁰ and contributions to dynamics such as zonal flows which feed back on I .²¹ In this paper, we work within the framework of a simple, single intensity field model. The applicability of such a model to the Dimits shift regime is somewhat questionable, as the Dimits shift is a regime of modest deviation from marginality and small zonal flow damping, so that zonal flow effects may be important. In the context of the present one-field model, the stabilizing effect of zonal flow-induced shearing (e.g., in the Dimits shift regime) can be absorbed into a shift (reduction) in $\gamma(x)$. A two-field model of turbulence spreading is a major undertaking, which is beyond the scope of this paper. In this section, detailed comparisons to our analytic theory are made for the cases, above the Dimits shift threshold, presented in Figs. 1, 3, and 4.

To pursue a study of turbulence spreading based on linear eigenmodes in toroidal geometry, one should consider a higher-order ballooning mode formalism.^{22,23} Note that the above equation manifests the crucial effect of spatial coupling in the nonlinear diffusion term. This implies that the integrated fluctuation intensity in a region of extent $2\Delta x$ about a point x [i.e., $\int_{x-\Delta x}^{x+\Delta x} I(x') dx'$] can grow, *even for negative* $\gamma(x)$, as long as $\chi(I) \partial I / \partial x|_{x-\Delta x}^{x+\Delta x}$ is *sufficiently large*. Alternatively, I can decrease, *even for positive* $\gamma(x)$, should $\chi(I) \partial I / \partial x|_{x-\Delta x}^{x+\Delta x}$ be *sufficiently negative*. Thus, the *profile* of fluctuation intensity is crucial to its spatiotemporal evolution,

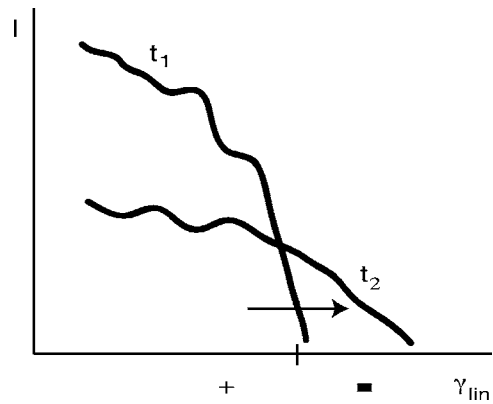


FIG. 5. A cartoon illustrating that the integrated fluctuation intensity in a region of extent $2\Delta x$ about a point x [i.e., $\int_{x-\Delta x}^{x+\Delta x} I(x') dx'$] can grow, *even for negative* $\gamma(x)$, as long as $\chi(I) \partial I / \partial x|_{x-\Delta x}^{x+\Delta x}$ is *sufficiently large*. Alternatively, I can decrease, *even for positive* $\gamma(x)$, should $\chi(I) \partial I / \partial x|_{x-\Delta x}^{x+\Delta x}$ be *sufficiently negative*.

as illustrated in Fig. 5. This notion can be further quantified by arguing by an analogy to tearing instability theory.²⁴ Integrating Eq. (1) in radius as described above, we obtain

$$\frac{\partial}{\partial t} \int_{x-\Delta x}^{x+\Delta x} dx' I(x', t) = \Delta'(I) I(x, t) + \int_{x-\Delta x}^{x+\Delta x} dx' [\gamma(x') I - \alpha I^{1+\beta}]. \quad (2)$$

Here, $\Delta'(I) \equiv \chi_0 (\partial / \partial x) I^\beta|_{x-\Delta x}^{x+\Delta x}$ characterizes the net flux of turbulence¹⁶ into (out of) $[x-\Delta x, x+\Delta x]$ via a net jump in the slope of fluctuation intensity. We recall that the classical tearing mode stability parameter Δ' , which characterizes the free energy in the equilibrium current gradient, is defined as a jump in the slope of perturbed flux function across the resistive layer.²⁴ Equation (2) clearly indicates that the *sign* of Δ' plays a crucial role for the growth of turbulence intensity. As illustrated in our previous work,⁸ simple relations $\gamma \sim \Delta'(I) / \Delta x$ and $\gamma_{\text{prop}} \sim U_x / \Delta x$ elucidate the physical meaning of $\Delta'(I)$ as the influx of turbulence intensity into the radial layer of width $2\Delta x$. It is also instructive to note that the tearing mode theory²⁴ predicts $\gamma \propto \eta^{3/5} \Delta'^{4/5}$, and the resistive layer width $\Delta x \propto \eta^{2/5} \Delta'^{1/5}$ which satisfies $\gamma \propto \Delta' \eta / \Delta x$, i.e., the magnetic flux is destroyed across the resistive layer at a rate proportional to $\eta \Delta'$.

These simple observations nicely illustrate the failure of the conventional local saturation paradigm,¹ and strongly support the argument that propagation of turbulence is a crucial, fundamental problem in understanding confinement scalings for fusion devices in which growth and damping rate profiles vary rapidly in space. Focusing on the weak turbulence regime, in which global gyrokinetic simulation results are well documented,¹⁵ we take $\beta=1$ for the rest of this paper.

We can make further analytic progress by considering profiles of $\gamma(x)$, α , and χ_0 which are constant in radius. Equation (1) is obviously a variant of the well-known Fisher-KPP (Kolmogoroff–Petrovsky–Piscounoff) equation for logistic-limited epidemic propagation,^{25,26} with nonlinear diffusion when $\gamma(x) > 0$. It is well-known that a reaction-diffusion-type equation including the Fisher-KPP equation

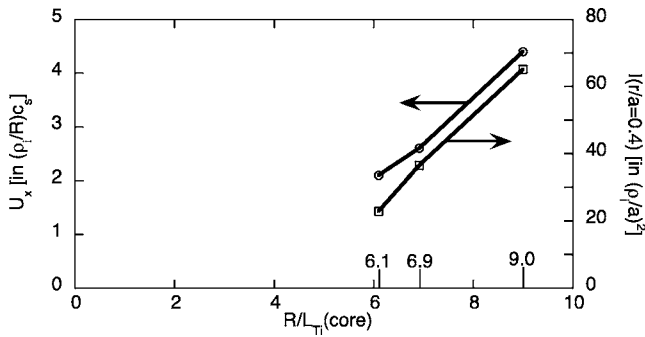


FIG. 6. Dependence of the front propagation speed and the time-averaged value (during the last 1/3 of the simulation duration) of the fluctuation intensity at $r/a=0.4$ on the ion temperature gradient.

exhibits a *ballistically* propagating front solution. Both analytic and numerical solutions have been presented in detail in Ref. 16. The front velocity is simply given by $U_x = \sqrt{\gamma^2 \chi_0 / 2\alpha}$. This solution indicates that the dynamics of $I(x,t)$ developing from a localized source of turbulence evolves in two steps. First, there is a rapid growth to local saturation at $I = \gamma(x)/\alpha$. Second, the value $I = \gamma(x)/\alpha$ defines an effective value of the intensity-dependent fluctuation diffusion $\chi = \chi_0 I = \chi_0 \gamma / \alpha$. A classic Fisher-KPP front with velocity $U_x = \sqrt{\gamma \chi / 2}$ is a consequence of the spatial coupling induced by a combination of local turbulence growth (with growth rate γ) and the effective diffusion ($\chi = \chi_0 \gamma / \alpha$). This front propagation on a hybrid time scale is a good example of a mesoscale phenomenon, which would be lost in a local or quasilocal model. It is crucial to note that the front of turbulence intensity can propagate ballistically (i.e., $x_{\text{front}} = U_x t$), even in the absence of toroidicity-induced coupling of neighboring poloidal harmonics. Therefore, the rapid propagation observed in simulations²⁷ does not imply the dominance of linear coupling of poloidal harmonics. Rather, rapid propagation should be considered as a more general consequence of the nonlinear dynamics. Since the scaling of U_x from our nonlinear theory (which increases with I and γ) is drastically different from the expectations from the one based on linear toroidal coupling,¹² our gyrokinetic simulations with the R/L_{Ti} scan provide crucial information on the dominant mechanism responsible for turbulence spreading. As shown in Figs. 1, 3, and 4, since the front propagation velocity changed significantly from $U_x \approx 2.1 \rho_i c_s / R$ to $U_x \approx 2.6 \rho_i c_s / R$, to $U_x \approx 4.2 \rho_i c_s / R$ as we increased the core gradient from $R/L_{Ti}=6.1$, to $R/L_{Ti}=6.9$ to $R/L_{Ti}=9.0$, our gyrokinetic simulation results [which approximately scale like $U_x \propto (R/L_{Ti})^{1.9}$] agree better with the scaling from a nonlinear diffusion model¹⁶ than with that from the linear toroidal coupling $U_x \propto \rho_i c_s / R$. These results are summarized in Fig. 6.

We also note that a numerical solution of Eq. (1) using the parameters in the simulations (the case with $R/L_{Ti}=6.9$ at the core) shows a spatiotemporal evolution of turbulence patches (Fig. 7) which is very similar to the simulation results shown in Fig. 1.

In the first significant numerical study addressing turbulence spreading which has been performed in the context of a global mode coupling analysis of toroidal drift waves,¹² it

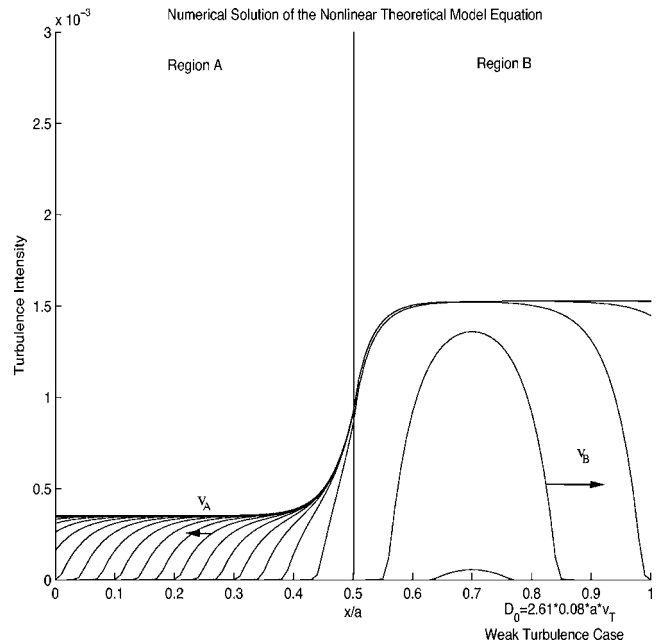


FIG. 7. Spatiotemporal evolution of the turbulence intensity from a numerical solution of Eq. (1) using the parameters used for GTC simulation in Fig. 1.

was observed that the linear toroidal coupling of different poloidal harmonics played a dominant role in the convective propagation of fluctuations into a region with a zero-level background of fluctuations in most parameter regimes. It is worthwhile to note that Ref. 12 was published before the important role of the self-generated zonal flows in regulating turbulence in toroidal geometry was fully realized.¹³ In a similar fashion to the way mean $\mathbf{E} \times \mathbf{B}$ flow shear causes decorrelation of turbulence in the radial direction,^{28,29} random shearing by zonal flows^{30,31} (which was not included in Ref. 12) would make linear toroidal coupling much weaker. This is shown by the measured reduction in the radial correlation length of the fluctuations³² as radially global toroidal eigenmodes are trimmed or destroyed by the zonal flows in gyrokinetic simulations.¹³ Thus, we believe that the ballistic front propagation observed in our gyrokinetic simulations should be considered as a more general consequence of the nonlinear dynamics, rather than as one due to linear toroidal coupling. We note that turbulence spreading has also been observed in the absence of toroidal coupling,^{33,34} and with temperature profile evolution.³⁵ Analytic studies of turbulence spreading have recently been extended to subcritical turbulence as well.³⁶

IV. CONCLUSION

The sum of these studies suggests that turbulence spreading is a simple, generic problem and not one due exclusively to toroidal geometry. An important element of the rationale for model building is to develop an analytic representation of turbulence spreading. Our results indicate the key importance of the fluctuation intensity profile and gradient in determining the spreading rate. This observation calls into question models which attempt to treat spreading by

averaging over a given region in an *ad hoc* manner.

The time-honored local saturation paradigm (i.e., $\gamma/k_{\perp}^2 = D$) is clearly inadequate and incomplete. A finite initial pulse of turbulence spreads on dynamically interesting time scales, and more rapidly than rates predicted by considerations of transport alone. For example, the predicted intensity velocity is the geometric mean of the local growth rate and the turbulent diffusivity. Efforts at modeling based on the local saturation paradigm should be reconsidered. Indeed, a recent finding³⁷ also indicates that flux-tube intuition based on the ballooning formalism is of dubious utility in describing mesoscale dynamics involving streamers. Since turbulence can tunnel into marginal or stable regions, fluctuation energy originating at the strongly turbulent edge may spread into the marginal core relatively easily, thus producing an intermediate region of strong turbulence. This phenomenon blurs the traditionally assumed distinction between the “core” and “edge” as some profiles from experiments indicate,³⁸ and suggests that the boundary between the two is particularly obscure in the *L* mode. It also identifies one element of the global profile readjustment which follows the *L*→*H* transition,^{39,40} namely, the quenching of turbulence in the core which originated at the edge. Application of this model has helped elucidate the dynamical connection between the core and edge, and the appearance of a connection zone, driven by the “spillover” of energy from the strongly turbulent edge into the quasimarginal core.

ACKNOWLEDGMENTS

One of the authors (P.H.D.) would like to thank Professor S.-I. Itoh for her hospitality at Kyushu University, where part of this work was completed. The authors would like to thank X. Garbet, R. J. Goldston, M. Greenwald, K. Itoh, S.-I. Itoh, Y. Kishimoto, E. J. Synakowski, W. M. Tang, L. Villard, M. Yagi, and F. Zonca, for useful discussions.

This work was supported by the U.S. Department of Energy Contract No. DE-AC02-76-CHO-3073 (PPPL), DOE Grant No. FG03-88ER 53275 (UCSD), DOE Cooperation Agreement No. DE-FC02-04ER54796 (UCI), and the US DOE SciDAC Center for Gyrokinetic Particle Simulation of Turbulent Transport in Burning Plasmas.

¹B. B. Kadomtsev, *Plasma Turbulence* (Academic, New York, 1965).

²P. H. Diamond and T. S. Hahm, *Phys. Plasmas* **2**, 3640 (1995).

³P. H. Diamond, S.-I. Itoh, K. Itoh, and T. S. Hahm, *Plasma Phys. Controlled Fusion* **47**, R35 (2005).

⁴K. H. Burrell, *Phys. Plasmas* **4**, 1499 (1997).

⁵E. J. Synakowski, S. Batha, M. Beer *et al.*, *Phys. Rev. Lett.* **78**, 2972 (1997).

⁶S.-I. Itoh and K. Itoh, *Plasma Phys. Controlled Fusion* **43**, 1055 (2000).

⁷T. S. Hahm, *Plasma Phys. Controlled Fusion* **44**, A87 (2002).

⁸T. S. Hahm, P. H. Diamond, Z. Lin, K. Itoh, and S.-I. Itoh, *Plasma Phys. Controlled Fusion* **46**, A323 (2004).

⁹Z. Lin and T. S. Hahm, *Phys. Plasmas* **11**, 1099 (2004).

¹⁰Z. Lin, S. Ethier, T. S. Hahm, and W. M. Tang, *Phys. Rev. Lett.* **88**, 195004 (2002).

¹¹B. B. Kadomtsev, *Plasma Phys. Controlled Fusion* **34**, 1931 (1992).

¹²X. Garbet, L. Laurent, A. Samain *et al.*, *Nucl. Fusion* **34**, 963 (1994).

¹³Z. Lin, T. S. Hahm, W. W. Lee, W. M. Tang, and R. B. White, *Science* **281**, 1835 (1998).

¹⁴A. M. Dimits, G. Bateman, M. A. Beer *et al.*, *Phys. Plasmas* **7**, 969 (2000).

¹⁵Z. Lin, T. S. Hahm, W. W. Lee, W. M. Tang, and P. H. Diamond, *Phys. Rev. Lett.* **83**, 3645 (1999).

¹⁶O. Gurcan, P. H. Diamond, T. S. Hahm, and Z. Lin, *Phys. Plasmas* **12**, 032303 (2005).

¹⁷E. J. Kim, P. H. Diamond, M. Malkov, T. S. Hahm, K. Itoh, S.-I. Itoh, S. Champeaux, I. Gruzinov, O. Gurcan, C. Holland, M. N. Rosenbluth, and A. Smolyakov, *Nucl. Fusion* **43**, 961 (2003).

¹⁸H. Sugama and M. Wakatani, *J. Phys. Soc. Jpn.* **61**, 3166 (1992).

¹⁹P. H. Diamond, V. B. Lebedev, D. E. Newman, B. A. Carerras, T. S. Hahm, W. M. Tang, G. Rewoldt, and K. Avinash, *Phys. Rev. Lett.* **78**, 1472 (1997).

²⁰D. E. Newman, B. A. Carerras, D. Lopez-Bruna, P. H. Diamond, and V. B. Lebedev, *Phys. Plasmas* **5**, 938 (1998).

²¹M. A. Malkov, P. H. Diamond, and M. N. Rosenbluth, *Phys. Plasmas* **8**, 5073 (2001).

²²F. Zonca, R. B. White, and L. Chen, *Phys. Plasmas* **11**, 2488 (2004).

²³R. B. White, L. Chen, and F. Zonca, *Phys. Plasmas* **12**, 057304 (2005).

²⁴H. P. Furth, J. Killeen, and M. N. Rosenbluth, *Phys. Fluids* **6**, 459 (1963).

²⁵R. A. Fisher, *Ann. Eugenics* **7**, 353 (1937).

²⁶A. Kolmogoroff, I. Petrovsky, and N. Piscounoff, *Clin. Cancer Res.* **1**, 1 (1937).

²⁷Y. Sarazin, X. Garbet, Ph. Ghendrih, and S. Benkadda, *Phys. Plasmas* **7**, 1085 (2000).

²⁸H. Biglari, P. H. Diamond, and P. W. Terry, *Phys. Fluids B* **2**, 1 (1990).

²⁹T. S. Hahm and K. H. Burrell, *Phys. Plasmas* **2**, 1648 (1995).

³⁰T. S. Hahm, M. A. Beer, Z. Lin, G. Hammett, W. W. Lee, and W. M. Tang, *Phys. Plasmas* **6**, 922 (1999).

³¹P. H. Diamond, M. Rosenbluth, F. L. Hinton, M. Malkov, J. Fleischer, and A. Smolyakov, *Proceedings of 17th International Conference on Fusion Energy*, Yokohama, 1998 (IAEA, Vienna, 1998), CD-ROM file TH3/1, <http://www-pub.iaea.org/MTCD/publications/PDF/csp-008c/fec-1998/html/node326.htm>

³²T. S. Hahm, K. H. Burrell, Z. Lin, R. Nazikian, and E.-J. Synakowski, *Plasma Phys. Controlled Fusion* **42**, A205 (2000).

³³L. Villard, S. J. Allfrey, A. Bottino *et al.*, *Nucl. Fusion* **44**, 172 (2004).

³⁴Y. Idomura, M. Wakatani, and S. Tokuda, *Phys. Plasmas* **7**, 3551 (2000).

³⁵L. Villard, P. Angelino, A. Bottino, S. J. Allfrey, R. Hatzky, Y. Idomura, O. Sauter, and T. M. Tran, *Plasma Phys. Controlled Fusion* **46**, B51 (2004).

³⁶K. Itoh, S.-I. Itoh, T. S. Hahm, and P. H. Diamond, *J. Phys. Soc. Jpn.* **74**, 2001 (2005).

³⁷Z. Lin, L. Chen, and F. Zonca, *Phys. Plasmas* **12**, 056125 (2005).

³⁸J. W. Hughes, D. A. Mossessian, A. E. Hubbard, B. LaBombard, and E. S. Marmor, *Phys. Plasmas* **9**, 3019 (2002).

³⁹J. G. Cordey, D. G. Muir, S. V. Neudatchin *et al.*, *Plasma Phys. Controlled Fusion* **36**, A267 (1994).

⁴⁰S. V. Neudatchin, T. Takizuka, H. Shirai *et al.*, *Plasma Phys. Controlled Fusion* **44**, A383 (2001).